Advances in Radiation Oncology (2016) **1**, 43-50

advances
in radiation oncology

www.advancesradonc.org

Scientific Article

Intravenous contrast-enhanced cone beam computed tomography (IVCBCT) of intrahepatic tumors and vessels

Cynthia L. Eccles BSc [a,b,*], Regina V. Tse MD [a,c], Maria A. Hawkins MD [a,b], Mark T. Lee MD [a,d], Douglas J. Moseley PhD [a], Laura A. Dawson MD [a]

[a] *Radiation Medicine Program, Department of Radiation Oncology, Princess Margaret Cancer Centre, University of Toronto, Toronto, Canada*
[b] *C.L.E. and M.A.H. are currently at the CRUK/MRC Oxford Institute for Radiation Oncology, University of Oxford, Oxford, United Kingdom*
[c] *R.V.T. is currently at the Department of Radiation Oncology, Chris O'Brien Lifehouse, Sydney, New South Wales, Australia*
[d] *M.T.L. is currently at Cancer Therapy Centre, Liverpool Hospital, University of New South Wales, Australia*

Received 18 November 2015; received in revised form 11 January 2016; accepted 19 January 2016

Abstract

Purpose: Liver tumors are challenging to visualize on cone beam computed tomography (CBCT) without intravenous (IV) contrast. Image guidance for liver cancer stereotactic body ablative radiation therapy (SABR) could be improved with the direct visualization of hepatic tumors and vasculature. This study investigated the feasibility of the use of IV contrast-enhanced CBCT (IV-CBCT) as a means to improve liver target visualization.

Methods and Materials: Patients on a liver SABR protocol underwent IV-CBCT before 1 or more treatment fractions in addition to a noncontrast CBCT. Image acquisition was initiated 0 to 30 seconds following injection and acquired over 60 to 120 seconds. "Stop and go" exhale breath-hold CBCT scans were used whenever feasible. Changes in mean CT number in regions of interest within visible vasculature, tumor, and adjacent liver were quantified between CBCT and IV-CBCT.

Results: Twelve pairs of contrast and noncontrast CBCTs were obtained in 7 patients. Intravenous-CBCT improved hepatic tumor visibility in breath-hold scans only for 3 patients (2 metastases, 1 hepatocellular carcinoma). Visible tumors ranged in volume from 124 to 564 mL. Small tumors in free-breathing patients did not show enhancement on IVCBT.

Conclusions: Intravenous-CBCT may enhance the visibility of hepatic vessels and tumor in CBCT scans obtained during breath hold. Optimization of IV contrast timing and reduction of artifacts to improve tumor visualization warrant further investigation.

Sources of support: This work is funded in part by the National Cancer Institute of Canada and the Canadian Cancer Society.
Conflicts of interest: None.

* Corresponding author. c/o Radiotherapy, The Royal Marsden, Downs Road, Sutton, Surrey SM2 5PT United Kingdom.
E-mail address: cynthiaeccles@gmail.com (C.L. Eccles).

http://dx.doi.org/10.1016/j.adro.2016.01.001

Introduction

Stereotactic body radiation therapy (SABR) relies on accurate patient positioning and delivery of radiation to ensure the target receives the intended dose, while minimizing the dose to the surrounding normal tissues. Kilovoltage (kV) cone beam computed tomography (CBCT) allows volumetric images to be acquired with the patient in the treatment position at the treatment unit immediately before radiation therapy (RT) delivery.[1] Despite respiratory liver motion, which can range from 5 to 50 mm in the craniocaudal dimension,[2] kV CBCT for image guided RT (IGRT) of liver cancers is feasible.[3] However, because liver tumors are generally not visible without intravenous (IV) contrast, surrogates such as radiopaque markers,[4] prior transarterial chemoembolization sites, or the liver itself, are generally used for IGRT. Because changes in the size, shape, and position of tumors (and normal tissues) have been noted during treatment of liver cancers,[3] and motion and/or deformations seen in the liver may not be representative of the tumor,[5] there is uncertainty in use of standard surrogates for IGRT.

Direct visualization of the liver tumor itself on CBCT would allow tumor-to-tumor volumetric image guidance, which should improve accuracy of liver SABR. Because most liver tumors have similar CT attenuation to normal liver parenchyma, IV contrast is given to enhance visualization of hepatic tumors.[6] The relative differences in influx, washout, retention, and/or accumulation of IV contrast between tumor and normal tissues during dynamic contrast-enhanced (DCE) CT imaging is useful for liver tumor detection and characterization. During DCE CT, hypovascular tumors (eg, colorectal liver metastases), appear iso-dense during the arterial phase (approximately 30 seconds after injection onset) and hypodense during the portal-venous phase (approximately 60 seconds after injection onset). Hepatocellular carcinomas (HCCs) demonstrate enhancement during the arterial phase and washout (less intensity compared with the adjacent liver) in the venous and delayed phases (approximately 180 seconds after injection onset). In light of these imaging principles, IV-CBCT may enhance the visibility of intrahepatic tumors and vessels with a view to improved image-guided stereotactic body RT. This manuscript describes our initial experience with the use of multifraction IV-CBCT for liver SABR.

Methods and Materials

Patients and eligibility

All patients provided informed consent for this local research ethics board–approved protocol that investigated IV contrast during research CBCT acquisition. Eligible patients were 18 years of age or older, had Child-Pugh class A liver function, Karnofsky performance status greater than 60, normal creatinine (<109 μmol/L), and were planned to be treated with SABR. Ineligibility criteria included history of IV contrast allergy or reaction, known renal disease, or diabetes.

Patients were treated either in exhale breath-hold (BH) using the Active Breathing Control (ABC) device (Elekta, Crawley, UK), or free-breathing (FB) with or without abdominal compression using an in-house developed device described elsewhere.[7] Individualized motion management was based on liver tumor motion determined at simulation using kV fluoroscopy, respiratory sorted (4-dimensional [4D]) CT and cine MR imaging. SABR was delivered in 6 fractions as previously described.[8]

CBCT

Cone beam CT scans were initially acquired using an Elekta Synergy Research Platform (Elekta), composed of a conventional x-ray tube and flat panel detector (RID 1640; PerkinElmer, Wiesbaden, Germany), that uses a Kodak Fast Lanex scintillator (Gd2O2S:Tb) of thickness 133 mg/cm^2 mounted on the linear accelerator (Eastman Kodak, Rochester, NY). The central axis of the kV beam is perpendicular to the treatment megavoltage beam, sharing the same center of rotation. Following the first 5 IV CBCT scans, a commercially available linear accelerator equipped with kV CBCT (Synergy, Elekta Oncology Systems) was used. Scans acquired on the research platform used 120 kVp, approximately 1289 mAs (total), and 3.3 or 5.5 frames per second; those acquired on the Elekta Synergy system used 120 kVp, approximately 1008 mAs (total), and 650 projections per 360° rotation. On both systems, in-house modifications enabling the interruption of the CBCT acquisition by the radiation therapist was used to facilitate the acquisition of exhale BH only images in patients treated with ABC

with BHs shorter than the complete CBCT scan ("stop and go" CBCT).[3] Free-breathing scans were acquired in 1 continuous acquisition. A maximum of 2 IV-CBCTs were planned per patient, most commonly acquired at fractions 2 and 5. All images were acquired with the patient in the treatment position immediately before or following radiation therapy. IV access was gained before each IV-CBCT and following a 10-mL test dose of IV contrast (Visipaque; Amersham Health, Princeton, NJ), contrast was administered at rate 3 to 5 mL/second, 2 mL/kg to a maximum of 200 mL. Cone beam imaging was initiated 0 to 30 seconds following contrast injection and acquired over 60 to 120 seconds. Noncontrast CBCTs were acquired daily, with the patient in the treatment position, either before the IV-CBCT or following completion of radiation delivery.

Data analysis

The IV-CBCT images were reconstructed and analyzed using the Pinnacle v7.6b (Philips Medical, Madison, WI) treatment planning system (TPS), by a radiation oncologist with experience in both SABR liver treatment planning and CBCT evaluation. A liver-to-liver manual fusion with noncontrast CBCT scans from the same fraction and the planning CT was performed to ensure the tumor and vessel location was known in the CBCT scans, whether or not there was enhancement. Regions of interest (ROI) in tumor or vessel and normal surrounding liver were contoured on the IV-CBCT and corresponding noncontrast CBCT. Regions of interest were approximately 1 cm in diameter and chosen in as homogeneous regions as possible, not overlapping edges of tumor or vessels. The CT numbers (minimum, maximum, mean, and standard deviation) within the ROIs were determined using the TPS's CT number, which is automatically generated for any segmented ROIs. The absolute difference in mean CT numbers, between tumor/vessel and surrounding normal liver, was compared between the IV-CBCT and noncontrast CBCT and is represented by the formula adapted from Nung et al[9] (as presented in Siewerdsen et al[10]): Absolute difference $= CT_T - CT_B$. Where CT_T is the mean CT number tumor or vessel and CT_B is the mean CT number surrounding normal liver ROI, and SD is the standard deviation of the CT numbers within the ROI. The contrast-to-noise ratio (CNR) is the ability of an imaging modality to distinguish between various contrasts and the inherent noise within an image (eg, from imaging hardware or tissue). The CNR is represented by the formula:

$$CNR = \frac{|CT_T - CT_B|}{\sigma_B}$$

Results

Patient characteristics and IV CBCT details

Between July 2006 and May 2007, 7 patients consented to this protocol. Five patients had liver metastases (4 colorectal, 1 melanoma), 1 had metastatic cholangiocarcinoma, and 1 had HCC (Table 1).

In total, 12 IV-CBCT and routine noncontrast CBCT pairs were acquired. Some patients (n = 2) were not able to have a second IV-CBCT because of logistical reasons. Images were acquired in ABC BH for 3 patients on both occasions, FB on both occasions in 2 patients, FB with abdominal compression on 1 occasion for a single patient, and FB and voluntary BH on 1 occasion each for the final patient (Table 2). All patients received their total planned contrast volume as per protocol. Cone beam CT scans

Table 1 Patient characteristics

IV CBCT	Patient no.	Age	Sex	Disease	Total GTV volume (mL)[a]	No. of GTVs
1 2	1	53	F	Metastatic colorectal cancer	458.3	2
3	2	61	M	Metastatic colorectal cancer	123.9	1
4 5	3	74	F	Metastatic cholangiocarcinoma	10.5	3
6	4	75	M	Metastatic melanoma	62.7	3
7 8	5	55	M	Metastatic colorectal cancer	7.4	1
9 10	6	74	M	Metastatic colorectal cancer	66.3	1
11 12	7	61	M	Hepatocellular carcinoma	563.7	2

CBCT, cone beam computed tomography; F, female; GTV, gross tumor volume; IV, intravenous; M, male.

[a] For patients with multiple GTVs, this is the sum total of all visible on contrast-enhanced planning CT. For the purposes of the IV-CBCT the largest nonvascular thrombosis GTV was evaluated.

Table 2 Per-patient BH and FB IV-CBCT details

IV CBCT	Patient ID	Imaging system/ scan type	Contrast volume (mL)	Respiratory management	FB amplitude (cm)	Injection time	Total time (s)	Acquisition time (s)	No. BH	Tumor visible?	Vessel visible?
Per-patient BH IV-CBCT											
1	1	RP/FS	120	BH		−24	127	58	4	No	Yes
2		RP/FS	120	BH		0	155	58	5	Yes	Yes
4	3	RP/FS	120	BH		0	108	75	4	Yes	Yes
5		RP/FS	120	BH		0	99	75	4	Yes	Yes
8[a]	5	ES/HS	170	BH		0	263	101	6	No	No
11	7	ES/HS	140	BH	0.9	−8	117	60	4	Yes	Yes
12		ES/HS	140	BH		−9	118	60	4	Yes	Yes
Per-patient FB IV-CBCT											
3	2	RP/FS	135	FB	0.3	0	60	60		No	No
6	4	ES/HS	150	COMP	0.8	0	90	60		No	No
7	5	ES/HS	170	FB	2.0	0	117	117		No	No
9	6	ES/HS	100	FB	3.0	−9	129	120		No	No
10		ES/HS	100	FB		−10	130	120		No	No

BH, breath hold; CBCT, cone bean computed tomography; COMP, abdominal compression; ES, Elektra Synergy CBCT; FB, free breathing; FS, full scan (360° rotation); HS, half scan (200° rotation); IV, intravenous; RP, research platform.

[a] This patient is normally treated in FB and therefore had not received any BH training.

were acquired over 360° (n = 5), 200° (n = 7) with 686 (n = 4), 386 (n = 6), or 167 (n = 2) projections. Table 2 summarizes patient and imaging characteristics.

Breath-hold patients had stop and go CBCT scans, in which images were acquired only during repeat exhale BHs, with short interruptions of the CBCT between BHs. For the 7 BH IV-CBCTs, 5 were obtained with 4 repeat BHs (range, 4-6) per scan, with BH durations ranging from 8 to 20 seconds (Table 2). One patient (patient 5, scan 2) had difficulty with BH, and, because prolonged interruptions, the total scanning time was 263 seconds. There were no complications from the IV contrast.

The reproducibility of the liver and tumor position in exhale BH and FB has been validated by this group previously,[3,7,8,11-16] and as such is not the subject of the current work.

Qualitative image analysis

The IV-CBCT scans were initially assessed visually by an expert user (R.V.T.) in the Pinnacle TPS. Tumor was visible in 5 of 7 (71%) BH IV-CBCT scans and vasculature on 6 of 7 (86%) BH IV-CBCT scans. Tumor or vasculature was enhanced in 42% and 50% of the BH IV-CBCT scans, respectively. Figure 1 is a representative image of tumor and vasculature enhancement in BH IV-CBCT.

CNR changes between tumor or vasculature and the liver were only calculated in patients in which changes were visualized. Details of the tumor/vasculature visualization are summarized in Table 2. Although image 8 was attempted as a "stop and go" exhale BH scan, this was in a patient requiring long interruptions between image acquisition in preparation for each subsequent BH. In addition to liver tumor and hepatic vasculature, IV-CBCT showed considerable enhancement of kidney architecture (which could prove useful in kidney SABR, Fig 2).

Quantitative image analysis

Hepatic vasculature was visible with relative contrast enhancement in 6 BH IV-CBCT scans (3 patients, 2 metastases; 1 HCC). Contrast-to-noise ratio was calculated for all tumors and vessels visible by eye with a mean (range) of 4.85 (1.49-9.61) and 1.75 (0.22-3.52), respectively. The mean absolute difference in CT number between vessel and liver for IV-CBCT and noncontrast CBCT was 2.6% and 1.3%, respectively ($P < .05$).

Decreased tumor attenuation relative to the liver was seen in 5 BH IV-CBCT scans (3 patients, 2 metastases; 1 HCC). In the IV-CBCT scans demonstrating tumor enhancement, there was no delay from the start of contrast injection to the start of image acquisition; all images were acquired in the half-scan (200° rotation) format on the research platform imager and contrast was injected at a rate of 3 mL/second. The parameters for the scans on which vasculature alone was visualized were more variable (Table 2).

Discussion

In contrast to the early reports on respiratory correlated IV contrast-enhanced CT in the liver[17] and pancreas,[18] this is the first multipatient report on the feasibility of IV-CBCT for liver tumor visualization during SABR. Rodal et al reported a case study of a dog with a maxillary tumor that underwent 5 CBCT scans before and after administration

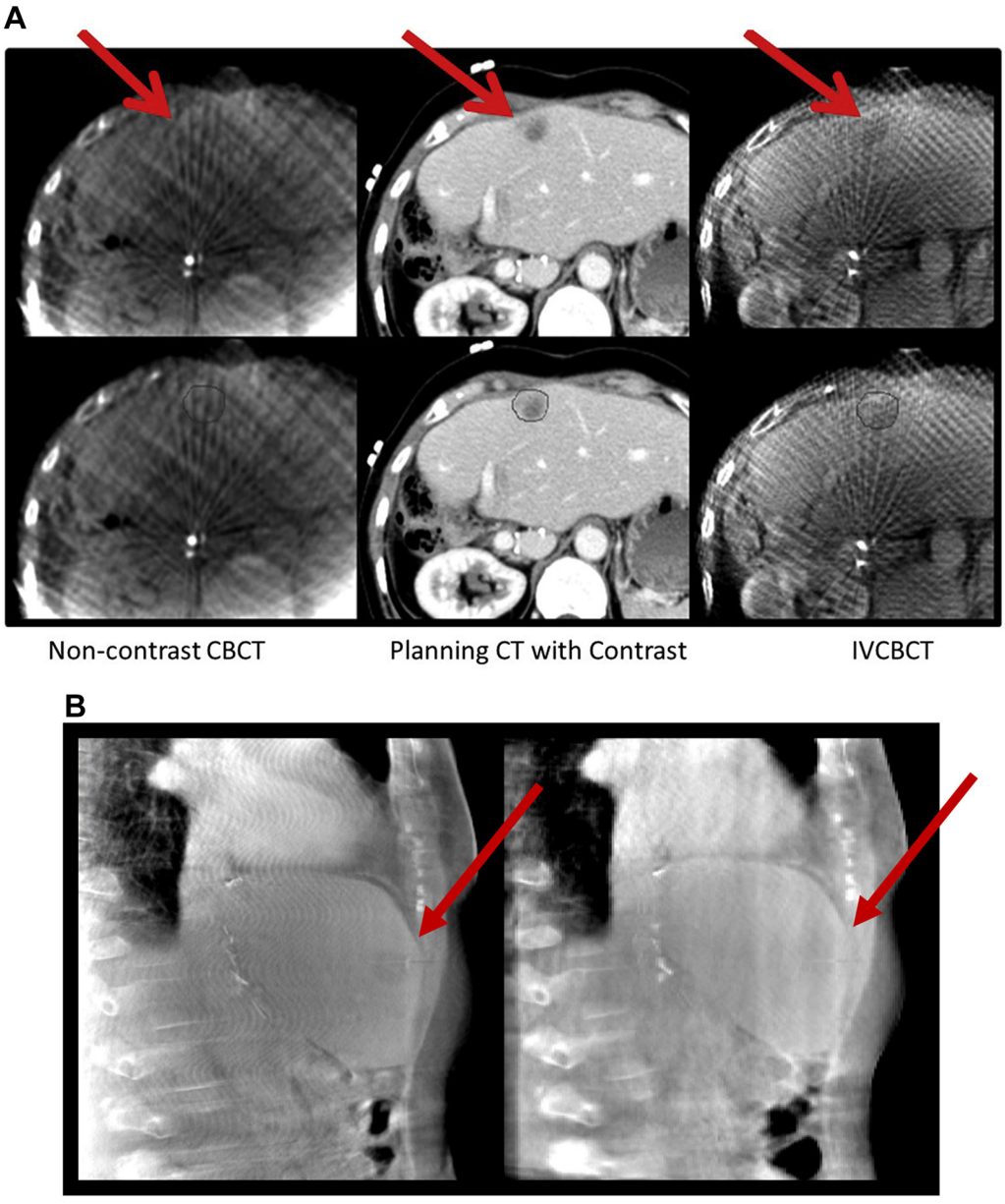

Figure 1 Intravenous cone bean computed tomography (IV-CBCT) images demonstrating tumor enhancement in patient 1. (A) Axial CT slices comparing noncontrast CBCT (left) with simulation CT (middle) and IV-CBCT (right) from a single fraction. Arrows indicate gross tumor volume (top) and gross tumor volume contour (black) from planning CT shown on bottom. Note the artifact from clips in the CBCTs. (B) Sagittal CBCT slices with (left) and without (right) IV contrast demonstrating tumor visibility with contrast.

of an iodinated contrast agent. The IV-CBCT scan demonstrates a more clearly discriminated tumor than does non contrast CBCT scan.[19] Improved target visualization in RT patients should improve accuracy of radiation delivery, by using the tumor for image guidance, instead of a surrogate. This is particularly beneficial in liver SABR, in which the tumor is not usually visible without IV contrast and surrogates for the tumor (eg, whole liver, a portion of the liver, inserted fiducial markers) are routinely used for IGRT and treatment is delivered on only a few fractions. Several authors[20,21] have reported on the successful use of surrogates such as fiducial markers; these are still surrogates and not the actual tumor. Should the actual visualization of the target be feasible on a day-to-day basis, this could potentially lead to more accurate tumor targeting. In the wake of adaptive RT, actual target visualization may prove more useful than the use of surrogates to modify treatments. In addition, fiducial marker implantation may not be suitable for all patients or, in some smaller centers, may require a delay because of availability of specialist staff to perform the implantation. As such, should IV-CBCT be available, this could prove an alternate option for patients undergoing short-course SABR. Intravenous-CBCT has proven useful in several non-RT applications such as neurovascular stent

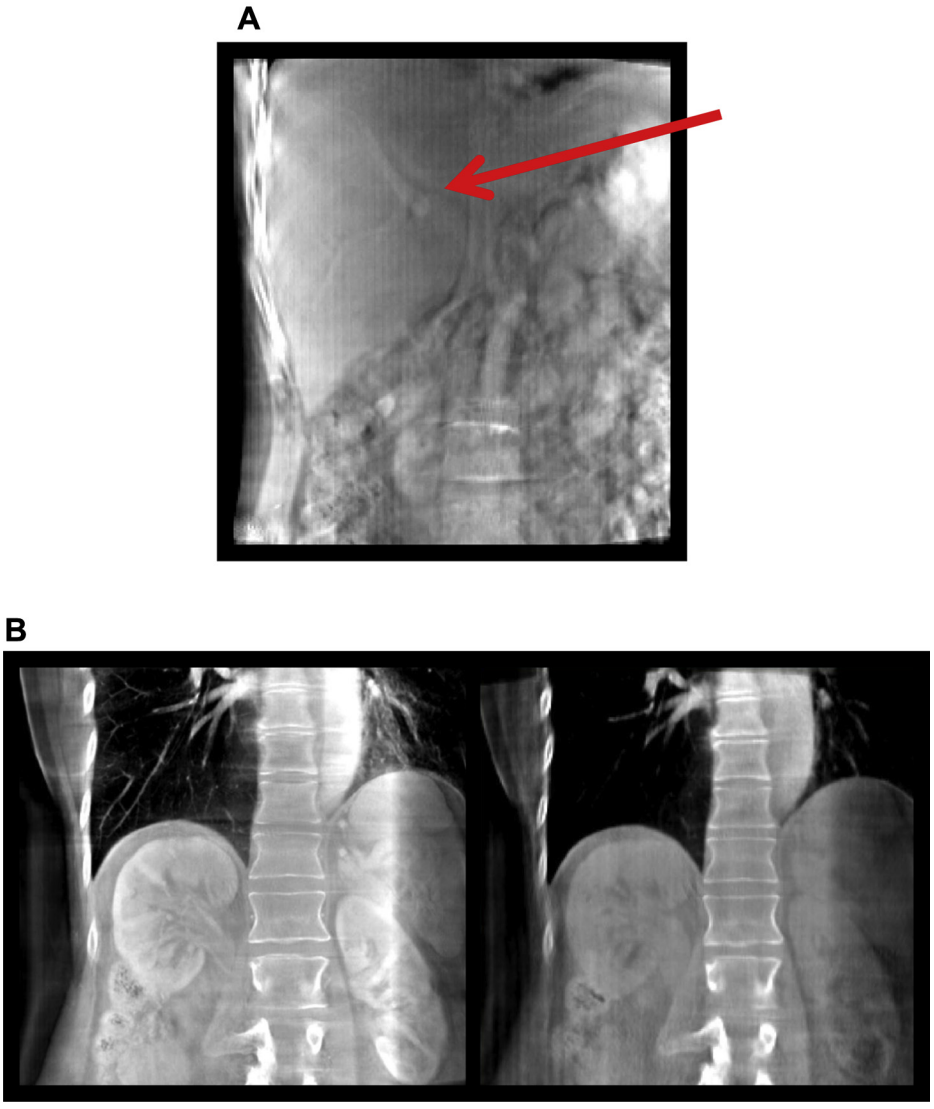

Figure 2 Intravenous cone bean computed tomography (IV-CBCT) images demonstrating normal tissue. (A) Coronal views of IV-CBCT demonstrating hepatic vasculature (patient 3). (B) Kidney architecture with (left) and without (right) IV contrast (patient 1).

visualization,[22] the detection of HCC during arterial portography,[23] abdominal interventional procedures such as angiography,[24] and intra-arterial cranial chemotherapy.[25] In attempts to optimize tumor/vasculature visualization on IV-CBCT, the procedure was modified over the course of the study; thus, it is not surprising that there was variable visualization of liver tumors and vasculature because the timing of contrast administration and scan acquisition is critical for target visualization on a helical contrast-enhanced CT.[6] Because all CBCT acquisitions were acquired over 1 to 2 minutes, the contrast had time to "wash-in" and "wash-out" of the tumor and vessels. If this dynamic process could be quantified, there is the potential for IV-CBCT to be used to measure perfusion, which is the focus of ongoing research.[26]

Most patients in this study had metastatic liver disease, which tends to be hypovascular and enhances best during the portal venous and delayed phases of conventional DCE CT, approximately 60 seconds following onset of injection. In the work presented here, all patients demonstrating tumor enhancement had metastatic liver cancers and a mean acquisition time of 65.6 seconds, meaning the scans were complete approximately in time with the venous uptake, avoiding washout. For the 2 metastatic BH IV-CBCT scans not demonstrating tumor enhancement, the acquisition times were >80 seconds, likely too late to capture the venous phase, but not late enough to demonstrate delayed enhancement (which would only be useful for primary liver cancers). However, further investigations are required to draw firm conclusions. Because of the length of time required for an IV-CBCT acquisition, it is likely that tumor enhancement will vary over time, with more predicted stability in the venous phase of

imaging (for metastases) or delayed phases of imaging (for primary liver cancers). It is possible that better visualization of the tumors would have occurred if the image quality was improved and/or with longer imaging over the delayed phases. It is hypothesized that, because of the time required for image acquisition, this application may be better suited to late enhancing tumors (eg, metastases) and/or tumors with sustained washout (eg, HCC). Furthermore, it is not unexpected that tumors were best seen on BH scans versus FB scans, and it is expected that with more modern CBCT (commercially available stop and go and 4D CBCT), the chances of IV contrast leading to tumor or vasculature visualization would be increased. The effects of IV contrast on megavoltage photon dosimetry have been studied by others,[27-29] who have determined the effects to be clinically insignificant. Because of the majority of the IV contrast would be washed out at the completion of the CBCT, it is unlikely that there would be a clinically significant effect of IV contrast on delivered doses.

As an alternative to IV-CBCT, which leads to transient target enhancement, there is motivation for a contrast agent that may demonstrate sustained enhancement over many radiation fractions. Nakagawa et al[30] reported on the injection of 3.5 mL lipiodol for this purpose in 2 patients (1 with brain metastases and 1 with HCC). When motion reduction/elimination is not feasible, alternate methods for improving online imaging should be used, such as respiratory correlated CBCT, described by Sonke et al.[31] At the time of this analysis, real-time respiratory correlated CBCT was not available. Retrospective respiratory correlation of noncontrast-enhanced CBCT scans has been used[32] and further optimization of respiratory correlated CBCT to eliminate artifacts in FB and compression patients may improve the potential for IV tumor localization for non-BH liver cancer SABR.

Although IV contrast can improve target and vessel visualization in BH liver SABR, the routine use of IV contrast over traditional RT courses may be associated with added risk, and this approach is only recommended for single or hypofractionated treatment schedules. Alternative (more complex and expensive) strategies for direct tumor visualization, such as magnetic resonance integrated treatment units, are being investigated and may improve accuracy of direct tumor localization in these patients.[33]

Conclusion

Intravenous contrast can enhance visualization of liver vasculature and tumors in BH CBCT, but not in FB CBCT, for the CBCT techniques investigated. Intravenous CBCT has the potential to improve direct tumor targeting during liver IGRT.

Acknowledgments

The authors gratefully acknowledge Andrea Marshall, CMD, for her assistance in the clinical implementation of this work, and Jeff Siewerdsen, PhD, for his helpful discussion regarding analyses.

References

1. Jaffray DA, Siewerdsen JH, Wong JW, Martinez AA. Flat-panel cone-beam computed tomography for image-guided radiation therapy. *Int J Radiat Oncol Biol Phys*. 2002;53:1337-1349.
2. Balter JM, Dawson LA, Kazanjian S, et al. Determination of ventilatory liver movement via radiographic evaluation of diaphragm position. *Int J Radiat Oncol Biol Phys*. 2001;51(1):267-270.
3. Hawkins MA, Brock KK, Eccles C, Moseley D, Jaffray D, Dawson LA. Assessment of residual error in liver position using kV cone-beam computed tomography for liver cancer high-precision radiation therapy. *Int J Radiat Oncol Biol Phys*. 2006;66:610-619.
4. Beddar AS, Kainz K, Briere TM, et al. Correlation between internal fiducial tumor motion and external marker motion for liver tumors imaged with 4D-CT. *Int J Radiat Oncol Biol Phys*. 2007;67:630-638.
5. Kirilova A, Lockwood G, Choi P, et al. Three-dimensional motion of liver tumors using cine-magnetic resonance imaging. *Int J Radiat Oncol Biol Phys*. 2008;71:1189-1195.
6. Baron RL. Understanding and optimizing use of contrast material for CT of the liver. *AJR Am J Roentgenol*. 1994;163:323-331.
7. Eccles CL, Patel R, Simeonov AK, Lockwood G, Haider M, Dawson LA. Comparison of liver tumor motion with and without abdominal compression using cine-magnetic resonance imaging. *Int J Radiat Oncol Biol Phys*. 2011;79:602-608.
8. Dawson LA, Eccles C, Craig T. Individualized image guided iso-NTCP based liver cancer SBRT. *Acta Oncol*. 2006;45:856-864.
9. Ning R, Chen B, Yu R, Conover D, Tang X, Ning Y. Flat panel detector-based cone-beam volume CT angiography imaging: System evaluation. *IEEE Trans Med Imaging*. 2000;19:949-963.
10. Schafer S, Stayman JW, Zbijewski W, Schmidgunst C, Kleinszig G, Siewerdsen JH. Antiscatter grids in mobile C-arm cone-beam CT: Effect on image quality and dose. *Med Phys*. 2012;39:153-159.
11. Brock KK, Hawkins M, Eccles C, et al. Improving image-guided target localization through deformable registration. *Acta Oncol*. 2008;47:1279-1285.
12. Case RB, Moseley DJ, Sonke JJ, et al. Interfraction and intrafraction changes in amplitude of breathing motion in stereotactic liver radiotherapy. *Int J Radiat Oncol Biol Phys*. 2010;77:918-925.
13. Dawson LA, Eccles C, Bissonnette JP, Brock KK. Accuracy of daily image guidance for hypofractionated liver radiotherapy with active breathing control. *Int J Radiat Oncol Biol Phys*. 2005;62:1247-1252.
14. Eccles C, Brock KK, Bissonnette JP, Hawkins M, Dawson LA. Reproducibility of liver position using active breathing coordinator for liver cancer radiotherapy. *Int J Radiat Oncol Biol Phys*. 2006;64:751-759.
15. Eccles CL, Dawson LA, Moseley JL, Brock KK. Interfraction liver shape variability and impact on GTV position during liver stereotactic radiotherapy using abdominal compression. *Int J Radiat Oncol Biol Phys*. 2011;80:938-946.
16. Velec M, Moseley JL, Eccles CL, et al. Effect of breathing motion on radiotherapy dose accumulation in the abdomen using deformable registration. *Int J Radiat Oncol Biol Phys*. 2011;80:265-272.
17. Beddar AS, Briere TM, Balter P, et al. 4D-CT imaging with synchronized intravenous contrast injection to improve delineation of liver tumors for treatment planning. *Radiother Oncol*. 2008;87:445-448.
18. Mancosu P, Bettinardi V, Passoni P, et al. Contrast enhanced 4D-CT imaging for target volume definition in pancreatic ductal adenocarcinoma. *Radiother Oncol*. 2008;87:339-342.

19. Rodal J, Sovik S, Skogmo HK, Knudtsen IS, Malinen E. Feasibility of contrast-enhanced cone-beam CT for target localization and treatment monitoring. *Radiother Oncol*. 2010;97:521-524.
20. Seppenwoolde Y, Wunderink W, Wunderink-van Veen SR, Storchi P, Mendez Romero A, Heijmen BJ. Treatment precision of image-guided liver SBRT using implanted fiducial markers depends on marker-tumour distance. *Phys Med Biol*. 2011;56:5445-5468.
21. Wurm RE, Gum F, Erbel S, et al. Image guided respiratory gated hypofractionated stereotactic body radiation therapy (H-SBRT) for liver and lung tumors: Initial experience. *Acta Oncol*. 2006;45:881-889.
22. Patel NV, Gounis MJ, Wakhloo AK, et al. Contrast-enhanced angiographic cone-beam CT of cerebrovascular stents: Experimental optimization and clinical application. *AJNR Am J Neuroradiol*. 2011;32:137-144.
23. Miyayama S, Matsui O, Yamashiro M, et al. Detection of hepatocellular carcinoma by CT during arterial portography using a cone-beam CT technology: Comparison with conventional CTAP. *Abdom Imaging*. 2009;34:502-506.
24. Hirota S, Nakao N, Yamamoto S, et al. Cone-beam CT with flat-panel-detector digital angiography system: Early experience in abdominal interventional procedures. *Cardiovasc Intervent Radiol*. 2006;29:1034-1038.
25. Ishikura R, Ando K, Nagami Y, et al. Evaluation of vascular supply with cone-beam computed tomography during intraarterial chemotherapy for a skull base tumor. *Radiat Med*. 2006;24:384-387.
26. Coolens C, Driscoll B, Dawson L. Feasibility study of 4D perfusion CT for hepatocellular carcinoma patients treated with radiation and sorafenib. *Practi Radiat Oncol*. 2013;3(2 Suppl 1):S29.
27. Rankine AW, Lanzon PJ, Spry NA. Effect of contrast media on megavoltage photon beam dosimetry. *Med Dosim*. 2008;33:169-174.
28. Nasrollah J, Mikaeil M, Omid E, Mojtaba SS, Ahad Z. Influence of the intravenous contrast media on treatment planning dose calculations of lower esophageal and rectal cancers. *J Cancer Res Therapeutics*. 2014;10:147-152.
29. Letourneau D, Finlay M, O'Sullivan B, et al. Lack of influence of intravenous contrast on head and neck IMRT dose distributions. *Acta Oncol*. 2008;47:90-94.
30. Nakagawa K, Yamashita H, Igaki H, Terahara A, Shiraishi K, Yoda K. Contrast medium-assisted stereotactic image-guided radiotherapy using kilovoltage cone-beam computed tomography. *Radiat Med*. 2008;26:570-572.
31. Sonke JJ, Zijp L, Remeijer P, van Herk M. Respiratory correlated cone beam CT. *Med Phys*. 2005;32:1176-1186.
32. Case RB, Sonke JJ, Moseley DJ, Kim J, Brock KK, Dawson LA. Inter- and intrafraction variability in liver position in non-breath-hold stereotactic body radiotherapy. *Int J Radiat Oncol Biol Phys*. 2009;75:302-308.
33. Lagendijk JJ, Raaymakers BW, Raaijmakers AJ, et al. MRI/linac integration. *Radiother Oncol*. 2008;86:25-29.